Yulianto Tejo Putranto[1,2], Oddy Virgantara Putra[3] , Isa Hafidz[5] , Tri Arief Sardjono[1] , Mochamad Hariadi[1] , Mauridhi Hery Purnomo[1,4]

Department of Electrical Engineering, Institut Teknologi Sepuluh Nopember (1), Universitas Katolik Soegijapranata (2), Department of Informatics, Universitas Darussalam Gontor (3), University Center of Excellence on Artificial Intelligence for Healthcare and Society (UCE AIHeS) (4), Department of Electrical Engineering, Institut Teknologi Telkom Surabaya (5)

doi:10.15199/48.2023.06.40

An Improved Performance of Support Vector Machine to Classify EEG Motor Imagery based on Differential Asymmetry

Abstract. *One challenge in EEG motor imaging is th e low signal-to-noise ratio of brain signals. Its emergence in the accurate rendition of brain signals varies significantly from person to person. Here, we propose a framework to classify tasks based on fusion features using a Support Vector Machine. Our features are acquired from Discrete Wavelet Transform and Empirical Mode Decomposition. Subsequently, the disparity between measurements of left and right brain signals was calculated. Our proposed work significantly improves accuracy from 83.29 % to 93.16 % compared to previous work.*

Streszczenie. *Jednym z wyzwań w obrazowaniu motorycznym EEG jest niski stosunek sygnału do szumu sygnałów mózgowych. Jego pojawienie się w dokładnym przekazywaniu sygnałów mózgowych różni się znacznie w zależności od osoby. Tutaj proponujemy ramy do klasyfikowania zadań w oparciu o funkcje fuzji przy użyciu maszyny wektorów nośnych. Nasze funkcje są uzyskiwane z dyskretnej transformacji falkowej i dekompozycji trybu empirycznego. Następnie obliczono rozbieżność między pomiarami sygnałów lewego i prawego mózgu. Nasza proponowana praca znacznie poprawia dokładność z 83,29% do 93,16% w porównaniu z poprzednią pracą*. (***Ulepszona wydajność maszyny wektorów nośnych do klasyfikacji obrazów motorycznych EEG w oparciu o asymetrię różnicową***)

Keywords: EEG Motor Imagery, Discrete Wavelet Transform, Empirical Mode Decomposition, Differential Asymmetry
Słowa kluczowe: EEG, Dyskretna Transformata Falkowa, asymeetria

Introductio

A brain-computer interface (BCI) is a system that allows a person to control a computer or other device using signals from their brain. This is typically done by recording electrical activity from the brain using electrodes placed on the scalp, and then using machine learning algorithms to interpret the brain signals and translate them into commands for the com puter. BCIs can be used for a variety of applications, includ ing communication and control of prosthetic devices, assis tive technology for people with disabilities, and neurofeed back for medical and therapeutic purposes. Brain-Computer Interface (BCI) is a system capable of translating brain activ ity represented by brain waves into commands or messages through interactive applications. The BCI system includes hardware and software used to manipulate brain signals to control a computer or other communication device. BCI al lows someone with physical limitations to interact with their environment. The waves or signals generated by the brain are used as a source of information. In general, the brain waves used are Electroencephalography (EEG) because of their non-invasive nature. Fig ‘1 shows the BCI closed loop system, which consists of six main stages: recording brain activity, pre-processing, feature extraction, classifica tion, translation into commands, and feedback [1, 2, 3].

The initial step after the EEG signal is obtained from the recording results is to filter the signal with a bandpass filter to reduce noise or artifacts and obtain an EEG signal in its frequency range. In several studies, the EEG signal is broken down with a sub-bandpass filter into EEG-forming frequency waves.

After obtaining the filtered EEG signal, in the process, feature extraction is then carried out. Several studies have been proposed to apply the autoregressive (AR) method, dis crete wavelet transforms (DWT), singular value decomposi tion (SVD), and typical spatial pattern (CSP) to obtain rel evant features in terms of the ability to distinguish between classes. These features provide high classification accuracy results [4, 5].

Our main contribution of this work is the incorporation of DWT and EMD to extract necessary features. From these features, we calculate the Differential Asymmetry. Subse quently, we finally impr

Related Work

Several methods are applied in machine learning mod els for classifying motor imagery b CSP method is the most widely used. Besides being used as a spatial filter, CSP is also used to select active segments to be processed by the classifier. The CSP method is also used to select features and electrode channels. [4, 6]. CSP is used for each EEG wave sub-band frequency to get fea tures. Apart from CSP, DWT method is often used for the decomposition of EEG signals [7, 8, 9]. The AR method is widely used as an initial process to support the following fea ture extraction process [10, 11, 12]. The evolutionary parti cle swarm optimization (PSO) algorithm selects features that significantly contribute to the classification process. PSO has been combined with fuzzy integral, which is used as a clas sifier [5]. Besides using DWT as signal decomposition, EMD decomposition has also been widely used in several studies [13, 14, 15, 16].

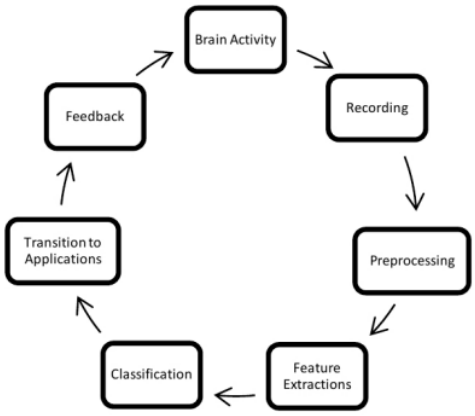

Fig. 1. Block diagram of a closed loop BCI system

In the classification process, several studies still use the classifier support vector machine (SVM) [8, 17, 18, 19, 20],

And a neural deep convolutional model network (CNN) has also been applied as a single experimental signal EEG clas sification for motor imaging. One of the activities that can be detected from the EEG signal is motor imagery, namely the state of a person imagining moving his motor organs, such as moving his left hand, right hand, feet, or tongue. Most imagi nary motor EEG signals are applied in BCI systems to control equipment, especially for neuromuscular disorders [21].

Alpha waves are a type of brain wave that are associ ated with a relaxed, awake state. They are typically observed in the 8-12 Hz frequency range and are most prominent over the occipital and parietal lobes of the brain. Alpha waves are often described as the brain's "default" state, and their activity tends to increase when a person is not focused on a particular task or stimulus. Some researchers have sug gested that alpha waves may play a role in the brain's "idling" or self-referential processes, such as daydreaming or mind wandering. Alpha waves are also often studied in the context of meditation and other practices that aim to promote relax ation and reduce stress. Alpha waves are produced in the posterior cortex, including the occipital, parietal, and poste rior temporal brain areas. Alpha waves have functional cor relations related to sensory, motor, and memory functions. Waves with a frequency range similar to alpha waves are mu waves, although there are physiological differences between the two. Mu waves are strongly associated with motor ac tivity and beta waves. The 12-25 Hz oscillations are often called beta wave activity. This frequency is generated in the posterior and frontal regions. Active, busy thinking or anxi ety and total concentration are generally known to correlate with higher beta levels. Across the middle cortex, beta lev els are more robust when a person is planning or moving, especially during grabbing or holding. This activity requires detailed movements of the fingers and concentration. The study related to beta waves is motor control. Beta waves ex perience desynchronization when carrying out actual move ments (motor execution) or imagining movements (motor im agery). These events are called event-related desynchro nization (ERD).

Beta waves are a type of brain wave that are associ ated with an alert, focused state of consciousness. They are typically observed in the 12-30 Hz frequency range and are most prominent over the frontal and central regions of the brain. Beta waves are typically dominant during tasks that require high levels of mental activity and concentration, such as problem-solving or decision-making. They are also as sociated with anxiety, stress, and other negative emotional states. In contrast to alpha waves, which are more prominent during relaxed, idle states, beta waves are typically more ac tive when a person is engaged in a demanding cognitive task. Meanwhile, after the movement, the beta wave will return to normal, or it is called event-related synchronization (ERS). This characteristic is then observed and used as input into the EEG-based BCI system [18]. Reference [22] shows that increasing the number of channels does not guarantee in creased classification accuracy. Therefore, there is an effort to make the number of channels used in EEG as small as possible. In [23], the EEG motor imagery channels that were widely used in the research were C3, C4, and Cz.

This paper uses an EEG-based BCI system to recog nize motor imagery activity by taking the difference in fea ture values between the measurements of left and right hemi sphere brain signals. This paper uses several statistical fea tures from the signal decomposition process using discrete wavelet decomposition (DWT) and empirical mode decom position (EMD). Because the right side of the brain controls the motor nerves of the left organ and vice versa, the EEG signals are generated by the right and left electrodes, which are different in certain imagery motor activities. This experi ment has been demonstrated in the ERD/ERS phenomenon. This difference is higher if the value of the disparity is sig nificant. This method, which enlarges the distance between the left and right hemisphere features, will be used as a new feature to increase the accuracy of the BCI system.

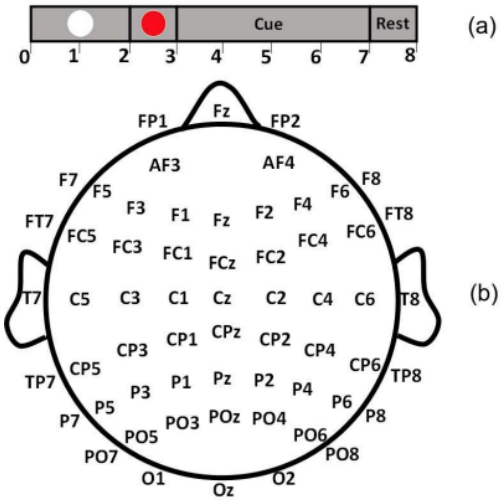

Fig. 2. Experimental archetype and the positions of electrode. (a) Experimental in one trial. (b) the positions of electrodes.

Material and Methods

Datasets

In this study, an open motor imagery EEG dataset was provided by Harvard Dataverse in the form of clean and mixed leg motor imagery EEG data [24]. This data is a multi class EEG motor imagery provided by Weibo Yi, et al, Tianjin University, China. The subjects contain ten persons, seven women, and three men. All of them are right-handed, around 23-25 years old. All subjects stated that they had no prior experience with motor imagery-based BCI. They must attend training for one week before recording the EEG. Subjects sat on a chair one meter apart in front of a computer screen. The duration of each trial is eight seconds. The first part is initi ated with a white dot in the center of the monitor that lasts for two seconds. In the 2nd second part, a red dot, a sign of preparation signal, appears on the monitor to recall the sub ject to be attentive to the following character indication. In the next three-second, the red dot vanished, and the char acter indication appeared on the monitor for four seconds. The respondents were inquired to focus on doing the motor imagery activity shown, 'Left Hand (LH)', 'Right Hand (RH)', 'Legs (F)', 'Both Hands (BH)', 'Left Hand & Legs'. Right (LH & RF)', 'Right Hand & Left Foot (RH & LF)'.

In the final task, 'Rest (R)' was conferred for one second prior to the next attempt (Fig. 2a). The experiment was sep arated into nine sections, with eight sections containing of 60 trials for all tasks. Furthermore, 10 trials for each imagination movement is in one section. Finally, one section consisting of 80 trials for the cooling-down state. The sequence of the motorized tasks was randomized. There are 5 to 10-minute breaks between sections. The total number of trials in the dataset for the study are 560.

The EEG signal is generated from 64 Ag/AgCl elec trodes attached to the scalp by the International 10/20 Sys tem. For reference, the nose and prefrontal lobes serve as ground (Fig. 1b). The Neuroscan SynAmps2

amplifier am plifies the EEG signal with a sampling rate of 1000 Hz and a band-pass filtering range of 0.5-100 Hz. In addition, there is an additional 50 Hz notch filter used during data acquisi tion to remove noise caused by 50 Hz grid waves. After that, the original EEG signal is band-pass filtered between 1 and 40Hz, then down-sampled at 200Hz. Prior to further analy sis, the typical average reference (CAR) is adopted here in pre-processing [25, 22].

The proposed method is shown in a flow chart in Fig. 3. After cleaning from noise and artifacts, the EEG signal is decomposed using DWT and EMD

Discrete Wavelet Transform

The Fourier Transform has the significant drawback of capturing global frequency information or frequencies present throughout the entire signal. Only a few applications, such as EEG, which uses data with brief intervals of recog nizable oscillation, may benefit from this signal breakdown. The Wavelet Transform is an alternate method that breaks down a function into a collection of wavelets. Then, we select a wavelet with a specific scale. Then, we move this wavelet throughout the entire signal, i.e., modify its location, multiply ing the wavelet and signal at each time step. We receive a coefficient for that wavelet scale at that time step as a result of this multiplication. The process is then repeated while in creasing the wavelet scale, such as with the red and green wavelets. The DWT is defined as

$$W_{\varphi}(j_0,k) = \frac{1}{\sqrt{M}} \sum_{x} f(x)\varphi_{j_0,k}(x) \tag{1}$$

$$W_{\Psi}(j,k) = \frac{1}{\sqrt{M}} \sum_{x} f(x)\Psi j,k(x) \tag{2}$$

The DWT method uses the Daubechies mother wavelet to decompose the EEG signal into parts according to fre quency. Since the sampling frequency is 200 Hz, the signal dataset is decomposed with a 5-level DWT. Coefficients ob tained CA1 (0-100 Hz), CD1 (101-200 Hz); CA2 (0–50 Hz), CD2 (51-100 Hz); CA3 (0–25 Hz); CD3 (26–50 Hz); CA4 (0-12 Hz), CD4 (13–25 Hz); CA5 (0–6 Hz), and CD5 (7–12 Hz). According to the task used, namely motor imagery, the results of the DWT are only taken for the D4 and D5 wave coefficients. These signals represent the EEG alpha and beta waves. Meanwhile, for EMD, IMF waves with low fre quency are taken. These waves will be calculated for their power values (rms), standard deviation, skewness, and kur tosis. These values are used

Empricial Mode Decomposition

Empirical mode decomposition (EMD) is a data-adaptive multi-resolution technique to decompose signals into compo nents according to their physical form. EMD can be used to analyze non-linear and non-stationary signals by separating them into components at different resolutions. EMD can be used to perform the time-frequency analysis while remaining in the time domain. The components are on the same time scale as the original signal, which makes it easier to analyze. Unlike wavelet analysis, EMD recursively extracts the differ ent resolutions from the data without using fixed functions or filters.

EMD has the ability to extract significant characteristics and patterns from a signal, and it can be beneficial when examining signals with non-stationary or intricate oscillatory patterns. It has been used to assess signals like sound, vi bration, and financial data in a number of disciplines, includ ing engineering, physics, and economi

EMD can be thought of as a fast oscillating signal su perimposed on a slower signal. Once the fast oscillations are extracted, the EMD algorithm treats the remaining slow components as a new signal and considers them fast os cillations superimposed on the slower components. The al gorithm continues until some stopping criterion is reached. The components in EMD are called intrinsic mode functions (IMF). An illustration of the EMD decomposition of the EEG signal is shown in Fig 1 and Fig 2.

The brain's work as a controller of motor movements in volves parts of the brain, in this case, the right and left hemi spheres of the brain. The left side of the brain and vice versa controls right-hand movement activity. The right side of the brain controls left-hand movement activity. It is this charac teristic that attempts to exploit to obtain features that distin guish tasks that involve right-hand and left-hand movements. There is a difference in these tasks. If the value of the differ ence between the two is taken, it sharpens the difference in value. This is what will be used as a feature. In the case of motor imagery, signals from electrodes C3, Cp3, and Fc3 are used, representing the brain's left hemisphere. Meanwhile, the right brain hemisphere is represented by signals from the C4, Cp4, and Fc4 electrodes. The difference from the value of each corresponding electrode feature, C3-C4, Cp3-Cp4, and Fc3-Fc4, is used as a new feature that will produce bet ter classifier accuracy.

There are four scenarios of how or the process of tak ing features compared. The first is the feature taken from the statistical values of the DWT results. Then, the features are fed to EMD to get their statistical value. Subsequently, the features from EMD and DWT were combined. Furthermore, the fourth is a modification of the third way by taking the fea ture difference value from a particular channel. In this case, it is called differential asymmetry, to be used as a new feature. Furthermore, the classification using SVM is carried out on the features used.

Feature Extraction

As explained in the previous section, the ERD/ERS phe nomenon, namely the EEG signal, experiences a decrease in stress when performing or imagining movement. With this in mind, the statistical feature will continue to be used. In this study, the statistical features used were standard deviation, skewness, kurtosis, and power signal (rms) values.

The average power and average absolute values of the Wavelet coefficients and IMFs were calculated as a feature. The use of the rms features, standard deviation, skewness, and kurtosis is also applied to the Wavelet coefficients as well as the IMF. Furthermore, the difference value for the channel symmetry pair will be sought from each statistical feature. These values will also be used as features. This feature of using the difference value of the pair of symmetrical channels has been applied in EEG research to detect emotion and is known as differential asymmetry.

Differential asymmetry is the value of the difference be tween two features, for example, the average power, as the results of measurements of the channel pair (electrode) is calculated as:

$$dx = x_l - x_r \tag{3}$$

where xl dan xr are the feature values of the left/right hemisphere symmetry pair (l, r) of the head. In the case of motor imagery, the channel pairs C3-C4, Cp3-Cp4, and Fc3- Fc4 were selected. Also included are the channels in the center, Cz and Cpz. This research will focus on the use of differential asymmetry as a feature marked "+DA". The re sults will be compared with the use of direct features without DA. SVM classifier is used as a classifier.

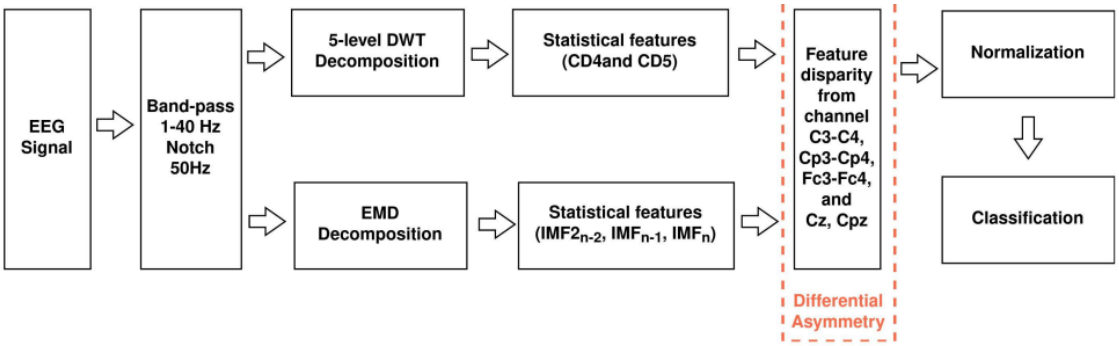

Fig. 3. Research method flowchar

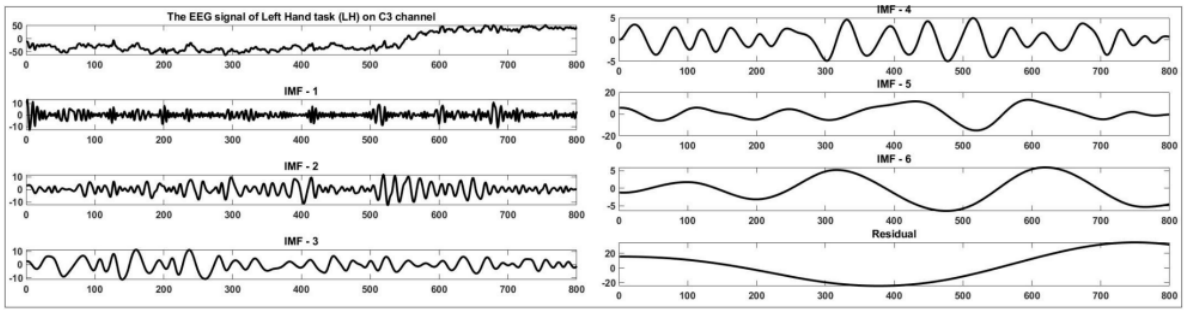

Fig. 4. An example of EEG signal decomposition using EMD. EEG signal subject S1 for task Left Hand, channel C3. Results of decomposition of IMF-1 to IMF-6 and Residues (bottom)

Experiments and Results

In this experiment, we utilized a computer with RAM 8 GB, Intel core i5. To classify seven types of mental tasks, and compare three types of multi-class CSP algorithms in Weibo Yi's research, the SVM classifier was used with Radial Basis Function (RBF) as the kernel.

Here, we collected the EEG dataset from [24]. The sig nals were decomposed by using DWT and EMD. These pro cesses work in parallel. DWT decomposed the signal into five levels which resulted in ten coefficients. Here, we set the N = 5 for the level, the DWT filter was set the db5 Daubechies wavelet. We picked only D4 and D5 waves.

On the other hand, EMD decomposed the input sig nal into three coefficients, IMFn−2, IMFn−1, and IMFn. Those decomposed waves were calculated with their statis tical features such as RMS, Standard Deviation, Skewness, and Kurtosis. From the DWT and EMD extracted coefficients, we measured the difference between the value from the pair ing channel. This disparity was calculated using Eq. 3. Here for EMD, we set the Sift Relative Tolerance to 0.2, Sift Max Iteration to 100, Maximum number of IMF to 10, maximum energy ratio to 20, and the interpolation method was set to Spline for smooth signal.

Table 1 shows the results of the SVM classifier accu racy for ten subjects with 10-Fold Cross Validation. In pre vious studies, the highest accuracy was obtained at 84.11% and an average accuracy of 70.43%. In this study, the av erage accuracy obtained using the DWT decomposition was 78.35%, while the highest accuracy value reached 88.57% tained is 80.94%, with the highest accuracy value of 89.82%. The average accuracy obtained by combining the DWT and EMD decomposition is 83.29%, while the highest accuracy value is 92.32%. By applying differential asymmetry (DA) to the combined DWT and EMD decomposition, the highest ac curacy value is 100%, and the average accuracy is 93.16%. Graphically it can be seen in Figure 6. As a comparison, the following is an example of the confusion matrix resulting from Subject S5 accuracy without applying DA and by applying DA as a feature, shown in Figure 6.

Discussion

From Weibo Yi's research, contralateral dominance was not observed during left-handed imagery. The same ERD pattern and spatial distribution during left-handed motor im agery were also revealed by investigations of four different MI tasks, which may be attributable to right-handed use. Imag inary leg movements desynchronize the alpha bands of not only the feet but also the hand representation areas, which are similar to those revealed by ERD maps on realistic head models during voluntary leg movements. Movement imagery desynchronizes the lower mu components somatotopically nonspecific, meaning desynchronization is present in all sen sorimotor areas (in both attended and unattended target ar eas). However, ERD of this wide leg area on the alpha band was only found in some subjects [25].

In addition, due to the simultaneous imagining of both hands, the bilateral hand areas are activated simultaneously. However, the situation is that the ERD is slightly weaker in the right hemisphere compared to the left hemisphere during both-handed imaginary processing, possibly associated with the right hand, i.e., more neurons have been activated in the right-handed region. In addition, the simultaneous imagin ing of the contralateral upper limb and lower limb certainly contributes to the simultaneous activation of the contralat eral hand area and the contralateral midfoot area. At the same time, the homolateral hand area is also activated due to its influence on the non-attended. Regions within the lower mu component. This phenomenon implies the possibility of applying compound limb motor imagery to rehabilitating pa tients suffering from severe motor injuries [25].

Table 1. Results of SVM classifier accuracy with several methods (in %)

Subject	S1	S2	S3	S4	S5	S6	S7	S8	S9	S10	mean
Multi-CSP [24]	70.82	81.79	63.14	64.28	67.85	74.11	71.61	68.93	71.96	66.25	70.07
Multi-GECSP [24]	70	80.54	63.14	62.32	65	73.75	73.39	66.07	72.5	60.54	68.73
Multi-sTRCSP [24]	73.67	84.11	62.07	64.64	66.07	75	75	68.75	71.07	63.93	70.43
Stat DWT	88.57	85.89	71.96	82.5	70	65.10	80	69.46	87.32	82.68	78.35
Stat EMD	82.32	87.32	75.71	81.43	74.29	74.08	79.11	77.68	87.68	89.82	80.94
Stat DWT+EMD	89.46	90	80.36	83.39	71.61	74.69	80.89	78.75	**92.32**	91.43	83.29
Stat DWT+EMD+DA	**90**	**100**	**84.46**	**89.29**	**99.82**	**100**	**89.29**	**100**	86.77	**91.96**	**93.16**

Table 2. The difference between the average LH and RH tasks for each feature and electrode

Feature	**Task**	**Channels**								
		C3	**C4**	**C3-C4**	**Cp3**	**Cp4**	**Cp3-Cp4**	**Fc3**	**Fc4**	**Fc3-Fc4**
RMS	LH	0.03	0.03	0.33	0.02	0.02	0.33	0.03	0.03	0.33
	RH	0	0.03	0.27	0.02	0.02	0.27	0.03	0.03	0.28
	Difference (LH-RH)	0	0	**0.05**	0	0	**0.06**	0	0	**0.05**
Standard deviation	LH	0	0	0.33	0	0	0.33	0	0	0.33
	RH	0	0	0.26	0	0	0.28	0	0	0.28
	Difference (LH-RH)	0	0	**0.06**	0	0	**0.06**	0	0	**0.06**
Skewness		0	0	0.33	0	0	0.33	0	0	0.33
	RH	0	0	0.28	0	0	0.28	0	0	0.28
	Difference (LH-RH)	0	0	**0.06**	0.6	0.63	**0.06**	0.64	0.64	**0.06**
Kurtosis	LH	0	0	0.33	0	0	0.33	0	0	0.33
	RH	0	0	0.28	0	0	0.28	0	0	0.28
	Difference (LH-RH)	0	0	**0.06**	0	0	**0.06**	0	0	**0.06**

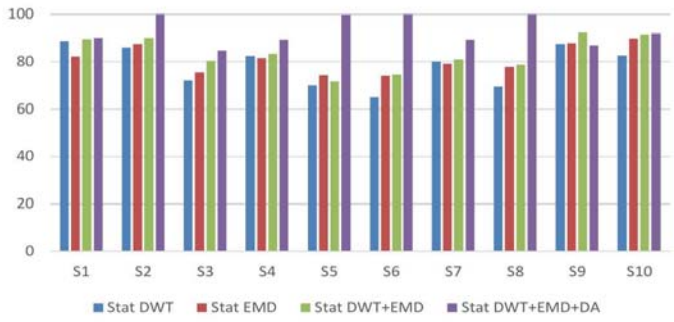

Fig. 5. Graph of the accuracy methods per subject (in %

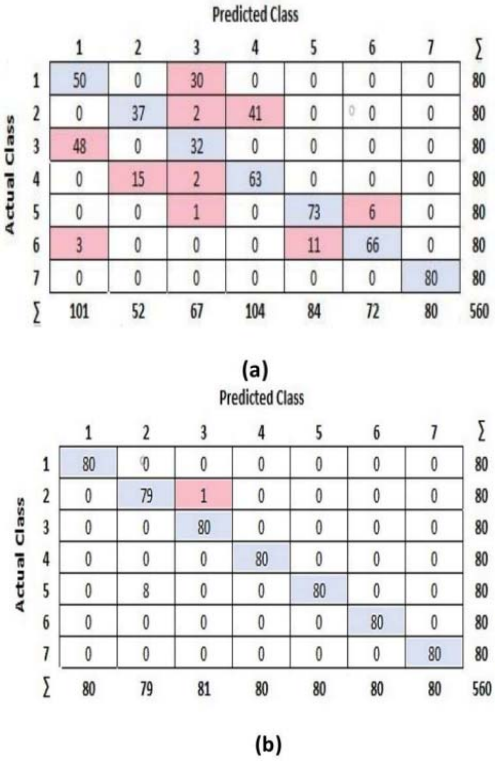

Fig. 6. Confusion matrix accuracy of Subject S5 (a)without applying DA (b) by applying DA

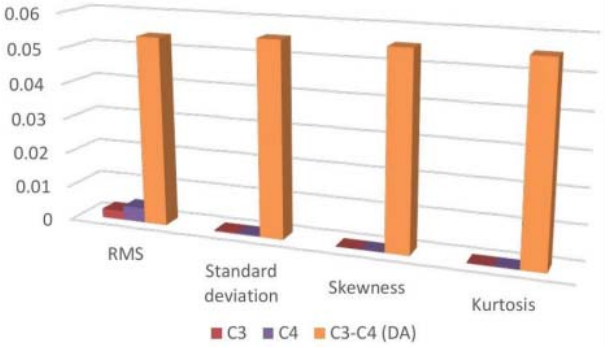

Fig. 7. Graph of the difference between the average LH and RH tasks for each feature in channel C3, C4 and C3-C4

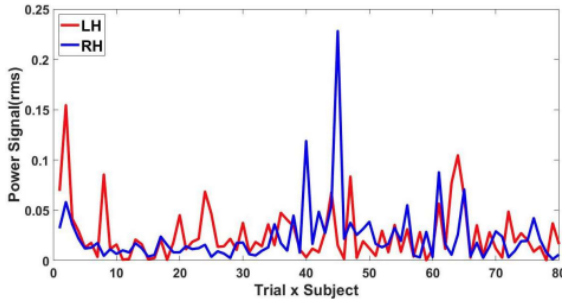

Fig. 8. Graph of average signal energy feature values for Subject-S5 in 80 trials left-hand (LH) and right-hand (RH) tasks channel C3

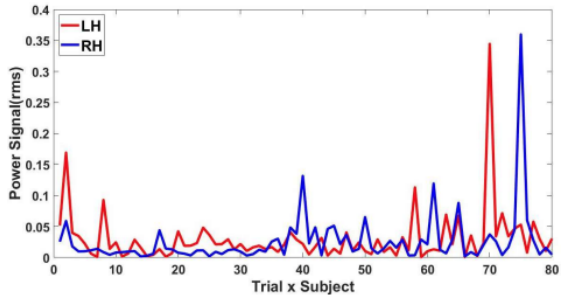

Fig. 9. Graph of average signal energy feature values for Subject-S5 in 80 trials left-hand (LH) and right-hand (RH) tasks channel C4

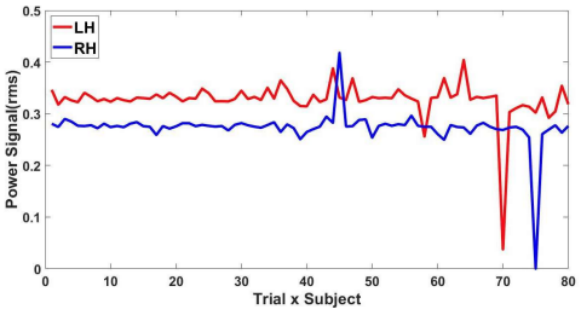

Fig. 10. Graph of average signal energy feature values for Subject S5 in 80 trials left-hand (LH) and right-hand (RH) tasks channel C3- C4.

In accordance with the objective, the difference in feature values between the electrode features and the difference in left and right hemisphere electrode features will affect the re sults of the accuracy of the SVM classifier. In this study, DA (differential asymmetry) values of C3-C4, Cp3-Cp4, and Fc3- Fc4 were used. Figures 8 and 9 show the power signal values for the left- and right-handed task motor imagery in C3 and C4 channels. Figure 10 shows the value of the difference in signal power for the two tasks between C3 and C4 channels. There is a significant difference between the two tasks if the differential asymmetry is taken. Table below shows the av erage difference between the two LH and RH tasks for each feature on channels C3, C4 and the differential asymmetry of the two channels. Graphically it can also be seen in Figure 7. There is a huge difference when compared between each channels C3, C4 with the difference between the channels C3-C4. This is in accordance with the feature selection rule.

The difference in the average scores of the two tasks shows that the use of the DA feature will increase the dis tance between classes. This can also be seen in the graphs of Figure 8 to Figure 19. Figure 8 - 10 show the differences in the power features (rms) of the LH and RH curves in 80 trials conducted by subject-S5. It can be seen in Figure 10, the distance between the LH and RH curves is greater than the distance between the LH and RH curves in Figures 8 and 9.

The same thing also happens to the other features, namely the standard deviation, skewness, and kurtosis. Compared to signal power, these statistical features show a tremendous difference (contrast) between using DA and with out DA. This can be seen in Figures 13, 16, 19, the distance between the LH and RH curves is greater than the distance between the LH and RH curves in Figure 10.

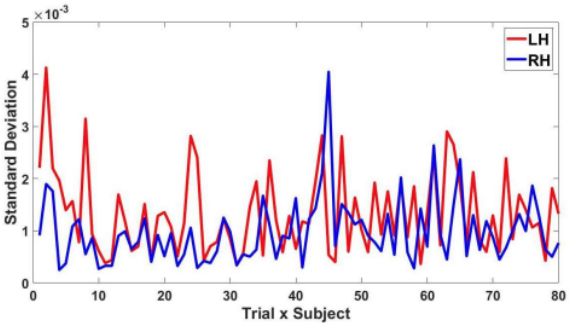

Fig. 11. Graph of standard deviation feature values of Subject-S5 in 80 trials for left-hand (LH) and right-hand (RH) tasks channel C3

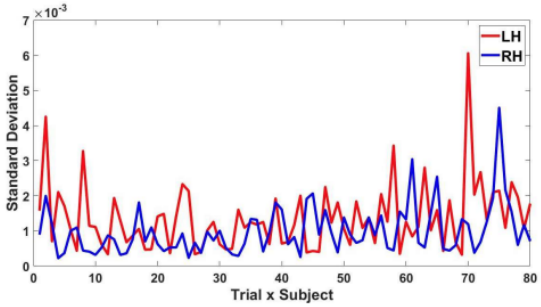

Fig. 12. Graph of standard deviation feature values of Subject-S5 in 80 trials for left-hand (LH) and right-hand (RH) tasks channel C4

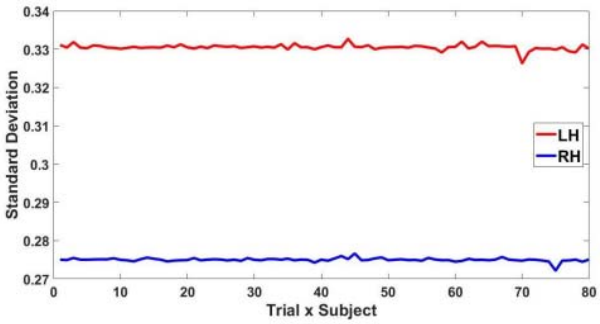

Fig. 13. Graph of standard deviation feature values of Subject-S5 in 80 trials for left-hand (LH) and right-hand (RH) tasks channel C3-C4

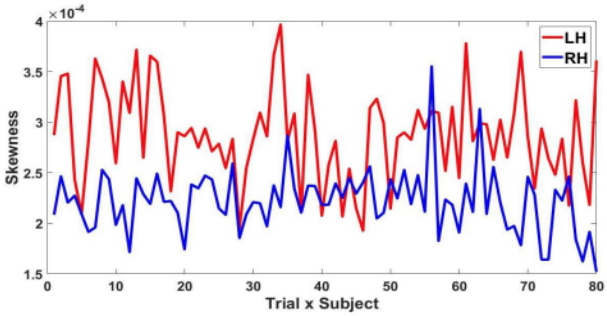

Fig. 14. Graph of skewness feature values of Subject-5 in 80 trials for left-hand (LH) and right-hand (RH) tasks channel C3

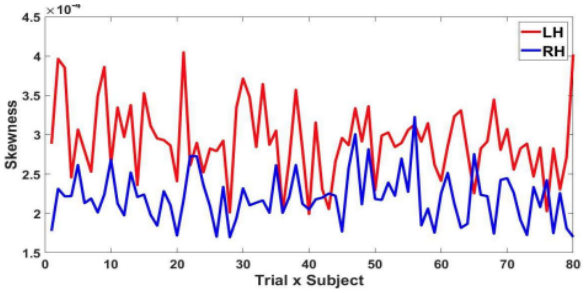

Fig. 15. Graph of skewness feature values of Subject-5 in 80 trials for left-hand (LH) and right-hand (RH) tasks channel C4

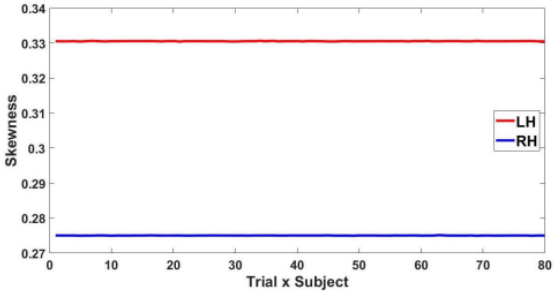

Fig. 16. Graph of skewness feature values of Subject-5 in 80 trials for left-hand (LH) and right-hand (RH) tasks channel C3-C4

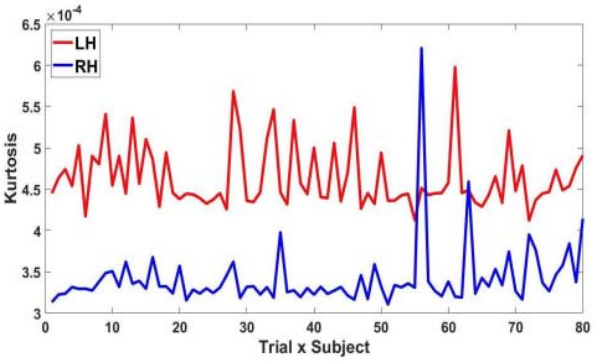

Fig. 17. Graph of kurtosis feature values of Subject-5 in 80 trials for left-hand (LH) and right-hand (RH) tasks channel C3

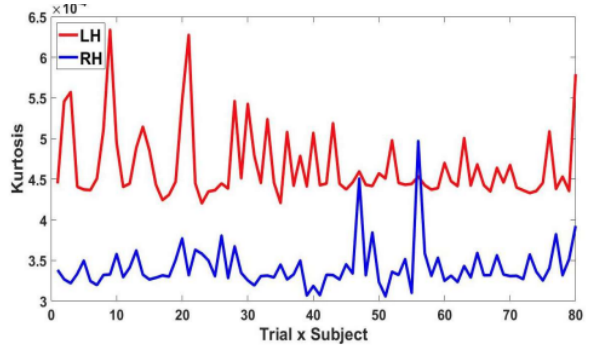

Fig. 18. Graph of kurtosis feature values of Subject-5 in 80 trials for left-hand (LH) and right-hand (RH) tasks C4 channels.

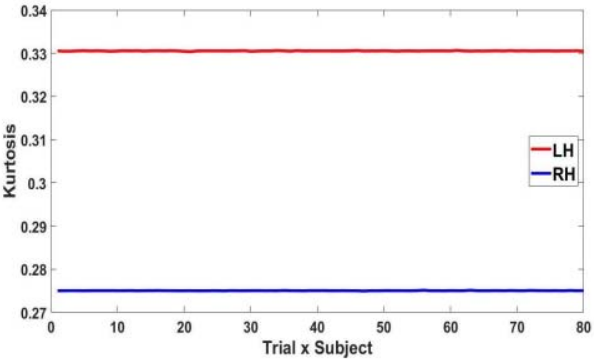

Fig. 19. Graph of kurtosis feature values of Subject-5 in 80 trials for left-hand (LH) and right-hand (RH) tasks channels C3-C4.

Conclusion

In this work, we investigated the use of motor imagery based on EEG. The dataset was gathered from a public repository that contains ten subjects. Our work comprises four scenarios. First, we employ the statistical feature of DWT. Next, the features were fed to EMD. Subsequently, those features were combined. Last, we extracted the fea ture disparity from a particular EEG channel using a tech nique called Differential Asymmetry. All of these features were classified using the SVM classifier. In here, we com pare our model with previous works, Multi-CSP, Multi-GECSP, Multi-sTRCSP, Stat DWT, Stat EMD, and Stat DWT+EMD. Our model achieved the best overall accuracy (OA) with a value of 93.16 %.

Authors: Yulianto Tejo Putranto, Department of Electri cal Engineering, Institut Teknologi Sepuluh No Teknik Mesin, Gedung B, C, dan AJ, Kampus ITS, Suko lilo, Surabaya, Indonesia, Postal Code 60111, email: yu lianto15@mhs.ee.its.ac.id, Oddy Virgantara Putra, Depart ment of Informatics, Universitas Darussalam Gontor, Jalan Raya Siman, Demangan, Siman, Ponorogo 63472, Indone sia, email: oddy@unida.gontor.ac.id, Isa Hafidz, Department of Electrical Engineering, Institut Teknologi Telkom Surabaya, Jalan Ketintang 156, Ketintang, Gayungan, Surabaya, In donesia, Postal Code 60231, email: isa@ittelkom-sby.ac.id, Tri Arief Sardjono, Department of Biomedical Engineer ing, Institut Teknologi Sepuluh Nopember, Jalan Teknik Mesin, Gedung B, C, dan AJ, Kampus ITS, Sukolilo 60111, Surabaya, Indonesia, Postal Code 60111, email: sard jono@bme.its.ac.id, Mochamad Hariadi, Department of Elec trical Engineering, Institut Teknologi Sepuluh Nopember, Jalan Teknik Mesin, Gedung B, C, dan AJ, Kampus ITS, Sukolilo 60111, Surabaya, Indonesia, Postal Code 60111, email: mochar@ee.its.ac.id, Prof. Mauridhi Hery Purnomo, Department of Electrical Engineering, Institut Teknologi Sepuluh Nopember, Jalan Teknik Mesin, Gedung B, C, dan AJ, Kampus ITS, Sukolilo 60111, Surabaya, Indonesia, email: hery@ee.its.ac.id, Yulianto Tejo Putranto, Univers tas Katolik Soegijapranata Semarang, Jalan Pawiyatan Luhur IV/1, Semarang 50234, Jawa Tengah, Indonesia, email: yu lianto@unika.ac.id

REFERENCES

[1] M. Clerc, L. Bougrain, and F. Lotte, Brain-computer interfaces 1: foundations and methods. ISTE ; Wiley, 2016. OCLC: ocn969907619.

[2] T. Prauzner, K. Prauzner, P. Ptak, H. Noga, P. Migo, and J. De pešová, “The influence of environmental conditions on the ac curacy of qeeg electroencephalography,” Przeglad Elektrotech niczny, vol. 96, pp. 86–89, 2020.

[3] S. Paszkiel, R. Rojek, N. Lei, and M. A. Castro, “Review of so lutions for the application of example of machine learning meth ods for motor imagery in correlation with brain-computer inter faces,” Przeglad Elektrotechniczny, vol. 97, pp. 111–116, 2021.

[4] M. Bentlemsan, E.-T. Zemouri, D. Bouchaffra, B. Yahya-Zoubir, and K. Ferroudji, “Random forest and filter bank common spatial patterns for eeg-based motor imagery classification,” pp. 235– 238, IEEE, 12 2014.

[5] S.-L. Wu, Y.-T. Liu, T.-Y. Hsieh, Y.-Y. Lin, C.-Y. Chen, C.-H. Chuang, and C.-T. Lin, “Fuzzy integral with particle swarm opti mization for a motor-imagery-based brain–computer interface,” IEEE Transactions on Fuzzy Systems, vol. 25, pp. 21–28, 12 2017.

[6] S.-M. Park, X. Yu, P. Chum, W.-Y. Lee, and K.-B. Sim, “Sym metrical feature for interpreting motor imagery eeg signals in the brain–computer interface,” Optik, vol. 129, pp. 163–171, 12 2017.

[7] W.-Y. Hsu, “Motor imagery electroencephalogram analysis us ing adaptive neural-fuzzy classification,” International Journal of Fuzzy Systems, vol. 16, 2014.

[8] M. ai Li, X. yong Luo, and J. fu Yang, “Extracting the nonlinear features of motor imagery eeg using parametric t-sne,” Neuro computing, vol. 218, pp. 371–381, 12 2016.

[9] S. U. Kumar and H. H. Inbarani, “Pso-based feature selection and neighborhood rough set-based classification for bci multi class motor imagery task,” Neural Computing and Applications, vol. 28, pp. 3239–3258, 12 2017.

[10] A. Subasi, A. Alkan, E. Koklukaya, and M. K. Kiymik, “Wavelet neural network classification of eeg signals by using ar model with mle preprocessing,” Neural Networks, vol. 18, pp. 985–997, 12 2005.

[11] H. Baali, A. Khorshidtalab, M. Mesbah, and M. J. E. Salami, “A transform-based feature extraction approach for motor imagery tasks classification,” IEEE Journal of Translational Engineering in Health and Medicine, vol. 3, pp. 1–8, 2015.

[12] S. Theodoridis and K. Koutroumbas, Pattern recognition. Aca demic Press, 4th ed ed., 2009.

[13] F. Ok and R. Rajesh, “Empirical mode decomposition of eeg signals for the effectual classification of seizures,” 12 2020.

[14] V. Bajaj and R. B. Pachori, “Eeg signal classification using em pirical mode decomposition and support vector machine,” 2012. Series Title: Advances in Intelligent and Soft Computing.

[15] A. Pradhan and M. I. of Technology-World Peace University, “A survey of classification of eeg signals using emd and vmd for epileptic seizure detection,” International Journal of Engineer ing Research and, vol. V9, p. IJERTV9IS050414, 12 2020.

[16] N. Zhuang, Y. Zeng, L. Tong, C. Zhang, H. Zhang, and B. Yan, “Emotion recognition from eeg signals using multidimensional information in emd domain,” BioMed Research International, vol. 2017, pp. 1–9, 2017.
[17] F. Lotte, M. Congedo, A. Lécuyer, F. Lamarche, and B. Ar naldi, “A review of classification algorithms for eeg-based brain–computer interfaces,” Journal of Neural Engineering, vol. 4, p. R1–R13, 12 2007.
[18] Q. Zhao, T. M. Rutkowski, L. Zhang, and A. Cichocki, “General ized optimal spatial filtering using a kernel approach with appli cation to eeg classification,” Cognitive Neurodynamics, vol. 4, pp. 355–358, 12 2010.
[19] Y. Yamasari, A. Qoiriah, N. Rochmawati, I. M. Suartana, O. V. Putra, and A. I. Nurhidayat, “Exploring the kernel on svm to enhance the classification performance of students’ academic performance,” pp. 42–46, Institute of Electrical and Electronics Engineers (IEEE), 12 2022.
[20] N. Z. Fanani, A. G. Sooai, K. Khamid, F. Y. Rahmanawati, A. Tormasi, L. T. Koczy, S. Sumpeno, and M. H. Purnomo, “Two stages outlier removal as pre-processing digitizer data on fine motor skills (fms) classification using covariance estimator and isolation forest,” International Journal of Intelligent Engineering and Systems, vol. 14, pp. 571–582, 12 2021.
[21] S. Sanei and J. A. Chambers, EEG Signal Processing and Ma chine Learning. Wiley, 2nd ed., 2022.
[22] G. K. Verma and U. S. Tiwary, “Multimodal fusion framework: A multiresolution approach for emotion classification and recogni tion from physiological signals,” NeuroImage, vol. 102, pp. 162– 172, 12 2014.
[23] M. K. M. Rahman and M. A. M. Joadder, “A review on the com ponents of eeg-based motor imagery classification with quanti tative comparison,” Application and Theory of Computer Tech nology, vol. 2, p. 1, 12 2017.
[24] Y. Weibo, “Eeg data of simple and compound limb motor im agery,” 2014.
[25] Z. Tang, S. Sun, S. Zhang, Y. Chen, C. Li, and S. Chen, “A brain-machine interface based on erd/ers for an upper-limb ex oskeleton control,” Sensors, vol. 16, p. 2050, 12 20